Journal of Organometallic Chemistry, 469 (1994) 45–53

Antimony(III) and phenylantimony(III) dimethyldithioarsinates: synthesis and mass spectral study. Crystal structure of $Ph_2SbS_2AsMe_2$, the first coordination polymer associated via bridging dimethyldithioarsinate ligands

D. Bryan Sowerby and Michael J. Begley

Department of Chemistry, University of Nottingham, Nottingham, NG7 2RD (UK)

Luminita Silaghi-Dumitrescu, Ioan Silaghi-Dumitrescu and Ionel Haiduc

Department of Chemistry, Babes-Bolyai University, RO-3400 Cluj-Napoca (Romania)

(Received August 4, 1993)

Abstract

Antimony(III) and phenylantimony(III) dimethyldithioarsinates, $Ph_nSb(S_2AsMe_2)_{3-n}$ with $n = 0$–2, have been prepared and characterized by their IR and FAB mass spectra and the structure of $Ph_2SbS_2AsMe_2$ has been determined by a single crystal X-ray diffraction study. The $Ph_2SbS_2AsMe_2$ molecular units are associated into a polymeric chain via S–$AsMe_2$–S bridging ligands, which connect approximately square pyramidal $SbPh_2S_2$ units, with essentially equal As–S interatomic distances (2.146 and 2.124 Å). A four-membered SbS_2As chelate ring is formed with short covalent (2.655 Å and long, semibonding (3.65 Å) antimony–sulfur contacts. The molecular units are interconnected by relatively short (2.830 Å) antimony–sulfur bonds to form a polymeric chain.

Key words: Antimony; Arsenic; X-ray diffraction; Mass spectrometry

1. Introduction

Ligands containing the S_2P groups are capable of showing a remarkable diversity of coordination patterns [1] and many crystallographic reports illustrate this [2]. In contrast, only five metal dithioarsinato complexes containing S_2As groups have been structurally investigated: $Me_2AsSAs(S)Me_2$ [3], $Zn_4S(S_2AsMe_2)_6$ [4], $Me_2Sn(S_2AsMe_2)_2$ [5], $Ph_2SbS_2AsPh_2$ [6] and $Me_3PtS_2AsMe_2$ [7]. Monodentate [3,5], anisobidentate [6] and bridging [4] coordination of the dithioarsinato groups have been found. Spectral data for a range of other Main Group metal dithioarsinates [5,8,9] also suggest that a broad variety of coordination patterns can be expected for these ligands.

Since we had previously investigated a number of antimony(III) and organoantimony(III) dithiophosphates and -phosphinates [10–12], further exploration of related dithioarsinates seemed worthwhile. We now report the synthesis of the title compounds and the crystal structure of $Ph_2SbS_2AsMe_2$, which displays the first polymeric structure involving –S–$AsMe_2$–S– groups as bridging ligands.

2. Experimental details

IR spectra were recorded in Nujol mulls using a Perkin-Elmer 983 spectrometer and FAB mass spectra with an MS 902 mass spectrometer.

2.1. Preparations

The starting materials, sodium dimethyldithioarsinate $NaS_2AsMe_2 \cdot 2H_2O$ [13], diphenylantimony(III)

Correspondence to: Dr. D.B. Sowerby or Dr. I. Haiduc.

0022-328X/94/$7.00
SSDI 0022-328X(93)24122-L

chloride [14] and phenylantimony(III) dichloride [14] were prepared by published methods. Diphenylantimony(III) dimethyldithioarsinate, $Ph_2SbS_2AsMe_2$, has been reported previously [6] being prepared from diphenylantimony(III) acetate.

2.2. *Antimony(III) tris(dimethyldithioarsinate), $Sb(S_2AsMe_2)_3$ (1)*

Freshly sublimed antimony(III) chloride (0.46 g, 2 mmol) dissolved in acetonitrile (15 ml) was treated with a solution of sodium dimethyldithioarsinate (1.37 g, 6 mmol) in the same solvent. The yellow precipitate formed was filtered off after 1 h and extracted with a 1:1 mixture of acetone and acetonitrile. Evaporation of the extract and the filtrate gave antimony(III) dimethyldithioarsinate (0.81 g, 64% yield) as a yellow crystalline solid, which was recrystallized from acetonitrile; m.p. 159°C. Anal. Found: C, 11.5; H, 2.9. $C_6H_{18}As_3S_6Sb$ calc. C, 11.5; H, 2.9%.

2.3. *Phenylantimony(III) bis(dimethyldithioarsinate), $PhSb(S_2AsMe_2)_2$ (2)*

Phenylantimony(III) chloride, $PhSbCl_2$ (0.54 g, 2 mmol) and sodium dithioarsinate (0.91 g, 4 mmol) each dissolved in 30 ml of acetonitrile, were mixed at room temperature. The precipitate of sodium chloride was filtered off and the filtrate concentrated *in vacuo*. The yellow crystals, which separated were filtered off and vacuum dried. Yield 0.32 g, 46%, m.p. 105°C. Anal. Found: C, 22.4, H, 3.2; $C_{10}H_{17}As_2S_4Sb$ calc.: C, 22.8, H, 3.4%.

2.4. *Diphenylantimony(III) dimethyldithioarsinate, $Ph_2SbS_2AsMe_2$ (3)*

A mixture of solutions of diphenylantimony(III) chloride, Ph_2SbCl (0.27 g, 0.86 mmol) and sodium dimethyldithioarsinate (0.20 g, 0.86 mmol), each in acetonitrile (20 ml), was stirred at room temperature for 2 h. The NaCl precipitate, and some unidentified yellow secondary products were filtered off. The filtrate was dried (Na_2SO_4) and the solvent evaporated to dryness, leaving yellow crystals, which were separated and recrystallized from acetonitrile. Yield 0.13 g, 45.7%, m.p. 124°C. Anal. Found: C 37.5, H 3.7; $C_{14}H_{16}AsS_2Sb$ calc.: C, 37.8; H, 3.6%.

2.5. *Structure of $Ph_2SbS_2AsMe_2$ (3)*

Crystals suitable for X-ray investigation were obtained by slow recrystallization from acetonitrile.

Crystal data. $C_{14}H_{16}AsS_2Sb$, $M = 445.0$, monoclinic, space group $P2_1/c$, $a = 9.688(2)$, $b = 9.903(2)$, $c = 19.347(6)$ Å, $\beta = 115.69(6)°$, $U = 1673.7$ Å^3, $Z = 4$, $D_c = 1.67$ g cm^{-3}, $F(000) = 860$, Mo K$_\alpha$ radiation, $\mu = 39.6$ cm^{-1}, crystal size $0.5 \times 0.25 \times 0.12$ mm^3.

TABLE 1. Atomic coordinates for $Ph_2SbS_2AsMe_2$ (with estimated standard deviations in parentheses)

Atom	x	y	z	U_{eq}
Sb(1)	0.11216(7)	0.35430(6)	0.33184(3)	0.0470
C(11)	−0.093(1)	0.2651(9)	0.3281(5)	0.0496
C(12)	−0.137(1)	0.278(1)	0.3881(7)	0.0636
C(13)	−0.279(1)	0.231(1)	0.3797(7)	0.0676
C(14)	−0.375(1)	0.164(1)	0.3132(8)	0.0747
C(15)	−0.330(1)	0.148(1)	0.2558(7)	0.0755
C(16)	−0.192(1)	0.200(1)	0.2619(6)	0.0623
C(21)	0.273(1)	0.2599(9)	0.4356(5)	0.0469
C(22)	0.237(1)	0.145(1)	0.4639(6)	0.0644
C(23)	0.346(2)	0.084(1)	0.5298(7)	0.0759
C(24)	0.491(2)	0.139(1)	0.5673(8)	0.0797
C(25)	0.527(1)	0.251(1)	0.5380(7)	0.0729
C(26)	0.420(1)	0.314(1)	0.4729(6)	0.0585
As(1)	−0.0930(1)	0.66006(9)	0.34959(5)	0.0473
S(1)	0.1067(3)	0.5498(2)	0.4245(1)	0.0511
S(2)	−0.1703(3)	0.6153(2)	0.2313(1)	0.0519
C(1)	−0.256(1)	0.621(1)	0.3769(7)	0.0670
C(2)	−0.042(2)	0.845(1)	0.3754(7)	0.0680

Structure determination. Data were measured for 3140 reflections of which 2310 with $I > 3\sigma(I)$ were considered observed and were corrected for Lorentz and polarization effects. Crystallographic calculations were carried out using the CRYSTALS programs [15] and scattering factors for neutral atoms [16]. An absorption correction was applied using DIFABS. Positions for the antimony and arsenic atoms were obtained using MULTAN [17] and the remaining atom positions by difference Fourier methods. Refinement was by full matrix least-squares with anisotropic thermal parameters for non-hydrogen atoms. Hydrogen atoms were placed at their calculated positions, but not refined in the final cycles. Refinement converged at R 5.6%, R_w 7.7% after application of a four coefficient Chebyshev weighting scheme. The final atomic coordinates are listed in Table 1. Tables of anisotropic thermal parameters and calculated hydrogen atom positions have been deposited with the Cambridge Crystallographic Data Centre. Structure factor listings can be obtained from D.B.S.

3. Results and discussion

The antimony(III) dimethyldithioarsinates $Ph_nSb(S_2AsMe_2)_{3-n}$ ($n = 0$–2) have been prepared as pale yellow solids from the corresponding antimony(III) chloride and sodium dimethyldithioarsinate as depicted in the following equation:

$$Ph_nSbCl_{3-n} + (3-n)NaS_2AsMe_2 \longrightarrow Ph_nSb(S_2AsMe_2)_{3-n} + (3-n)NaCl$$

The products are best recrystallized by slow evaporation of solutions in acetonitrile, since orange precipitates are often obtained when the solutions are heated. The compounds are stable for some weeks at room temperature under nitrogen but darken on more prolonged storage.

3.1. Infrared spectra

Bands characteristic of phenyl and dithioarsinate groups were observed in the expected spectral regions for all three compounds. For the dimethyldithioarsinato ligand, the most important region is that between 400 and 500 cm^{-1}, where arsenic–sulfur stretching vibrations are located [5,13,18]. The diagnostic bands for these groups are listed in Table 2. Structurally important conclusions cannot be drawn from the infrared spectra, except that it is clear that the ligand is not monodentate in any of the three compounds. Bands for a monodentate ligand are expected near 480 cm^{-1} (As = S) and 405 cm^{-1} (As–S) [15].

3.2. Mass spectra

The FAB mass spectrum of antimony(III) dimethyldithioarsinate (1) (see Scheme 1) shows a peak for the molecular ion ($m/z = 628$) and the major fragments are those resulting from the loss of dithioarsinato groups (S_2AsMe_2). Loss of neither methyl nor sulfur is observed from the parent ion and the first dithioarsinato group is lost intact. The two remaining dithioarsinato groups can each lose one sulfur, and methyl groups are lost from $[SbS_2Me_2]^+$ ($m/z = 258$) to form finally the smallest antimony-containing fragment. $[SbSAs]^+$ ($m/z = 228$). The FAB spectrum of phenylantimony(III) dimethyldithioarsinate (2) (see Scheme 2) is more complex, as the presence of a phenyl group increases the number of possible fragmentation routes. Phenyl and dithioarsinato group cleavage are both observed, with the $PhSb^+$ ion formed by elimination of either a dithio- or a monothioarsinato group. Fragments observed in the spectrum after cleavage of the phenyl groups are similar to those observed for the unsubstituted antimony(III) dimethyldithioarsinate.

TABLE 2. Infrared spectral data (cm^{-1})

Compound	ν(As=S)	ν(As–S)	ν(As–C)
$Sb(S_2AsMe_2)_3$	470s	440m	599m 621m
$PhSb(S_2AsMe_2)_2$	470s	429m	600m 621m
$Ph_2Sb(S_2AsMe_2)$	475sh 470s	422m	595m 622m

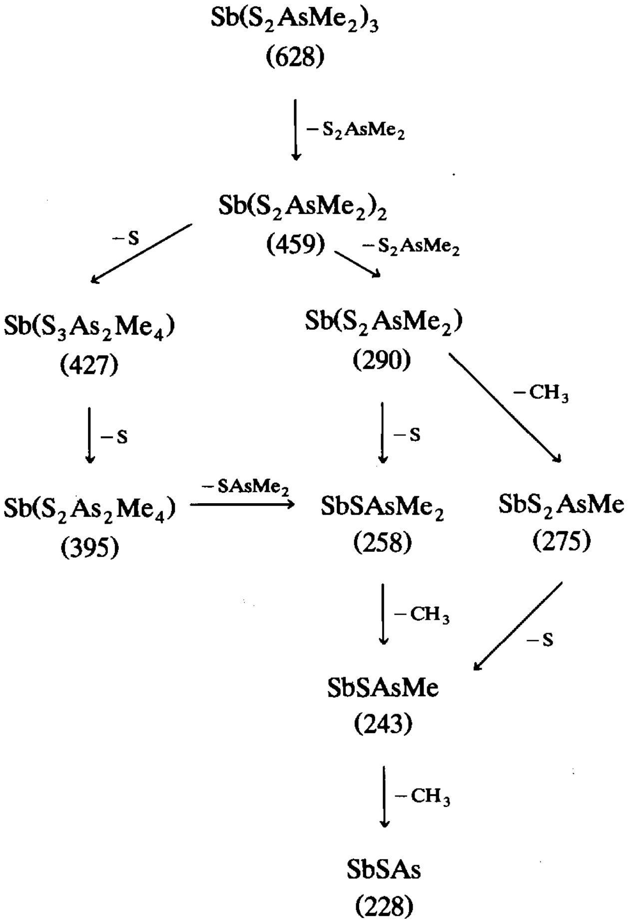

Scheme 1. FAB mass spectrum of $Sb(S_2AsMe_2)_3$.

A molecular ion peak ($m/z = 444$) is observed in the FAB spectrum of diphenylantimony(III) dimethyldithioarsinate (3) (see Scheme 3) and in this case there are three ways in which the parent ion can fragment, *viz.* cleavage of sulfur, methyl or phenyl. The first two processes are not very important, but loss of a phenyl group leads to $PhSb(S_2AsMe_2)$, the base peak of the spectrum. Monophenylantimony $PhSb^+$ and diphenylantimony, Ph_2Sb^+ ions are formed by successive loss of sulfur, methyl, thioarsenious and dithioarsinato groups, and formation of the heterocyclic ion $C_{12}H_{10}Sb^+$ from Ph_2Sb^+ by loss of two hydrogens is reflected in the isotopic ratios of the peaks with $m/z = 273/275/277$ (the m/z peak at 275 is shared by the two fragments, so the relative intensity of this peak is the sum of the peaks containing ^{121}Sb and ^{123}Sb isotopes. Fragmentation of dimethyldithioarsinato groups is common to all three compounds and is summarized in Scheme 4.

A number of ions result from collision processes within the mass spectrometer, among which are: $[Me_3As]^+$ ($m/z = 120$), $[AsSAsMe]^+$, ($m/z = 197$), $[Me_2S]^+$ ($m/z = 212$), $[Me_3As_2S]^+$ ($m/z = 227$), $[Me_4As_2S]^+$ ($m/z = 242$), $[Me_4As_2S_2]^+$ ($m/z = 274$).

The relative intensities of the antimony containing peaks observed in the mass spectra are given in Table 3.

3.3. Structure of $Ph_2SbS_2AsMe_2$ (3)

The structure of the basic unit in **3** is shown in Fig. 1, which also gives the atom numbering scheme. The compounds is, however, associated in the solid state, giving a structure which is unique in being the first coordination polymer associated through dithioarsinato ligands. A diagram showing this association, which leads to infinite chains along the *b* axis, is given in Figure 2. Important molecular parameters are summarized in Table 4. A four-membered chelate ring SbS_2As is formed within the molecular unit, which involves a short Sb(1)–S(1) bond (2.655 Å) and a secondary intramolecular Sb(1)...S(2) interaction (3.652 Å). The monomeric $Ph_2SbS_2AsMe_2$ units are then connected into a polymeric chain via intermolecular Sb(1)–S(2′) bonds (2.830 Å), which are only slightly longer than the primary Sb(1)–S(1) bonds in the chelate ring, but within the range of the covalent bond interatomic distances. These values are to be compared with the sums of covalent radii (2.45 Å) [19] and van der Waals radii (3.92 Å) [20] for antimony and sulfur. The intramolecular secondary Sb(1)–S(2) distance (3.652 Å) is shorter than the sum of van der Waals radii but longer than the sum of the intramolecular non-bonded atomic radii (2.45 Å) [21]. The arsenic–sulfur interatomic distances are very similar in length (2.124 and 2.146 Å) falling between those for single (*ca.* 2.20 Å) and double (*ca.* 2.05 Å) bonds. For example, the arsenic–sulfur single

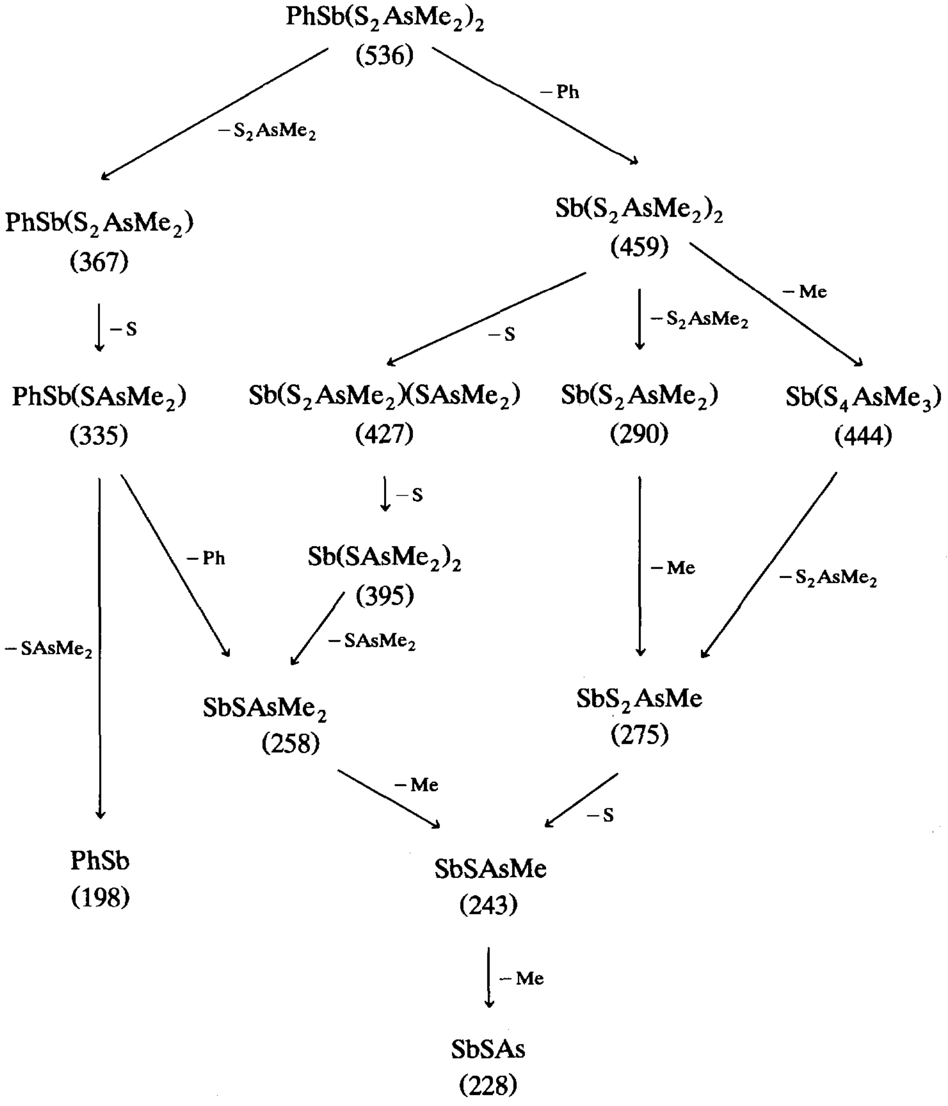

Scheme 2. FAB mass spectrum of $PhSb(S_2AsMe_2)_2$.

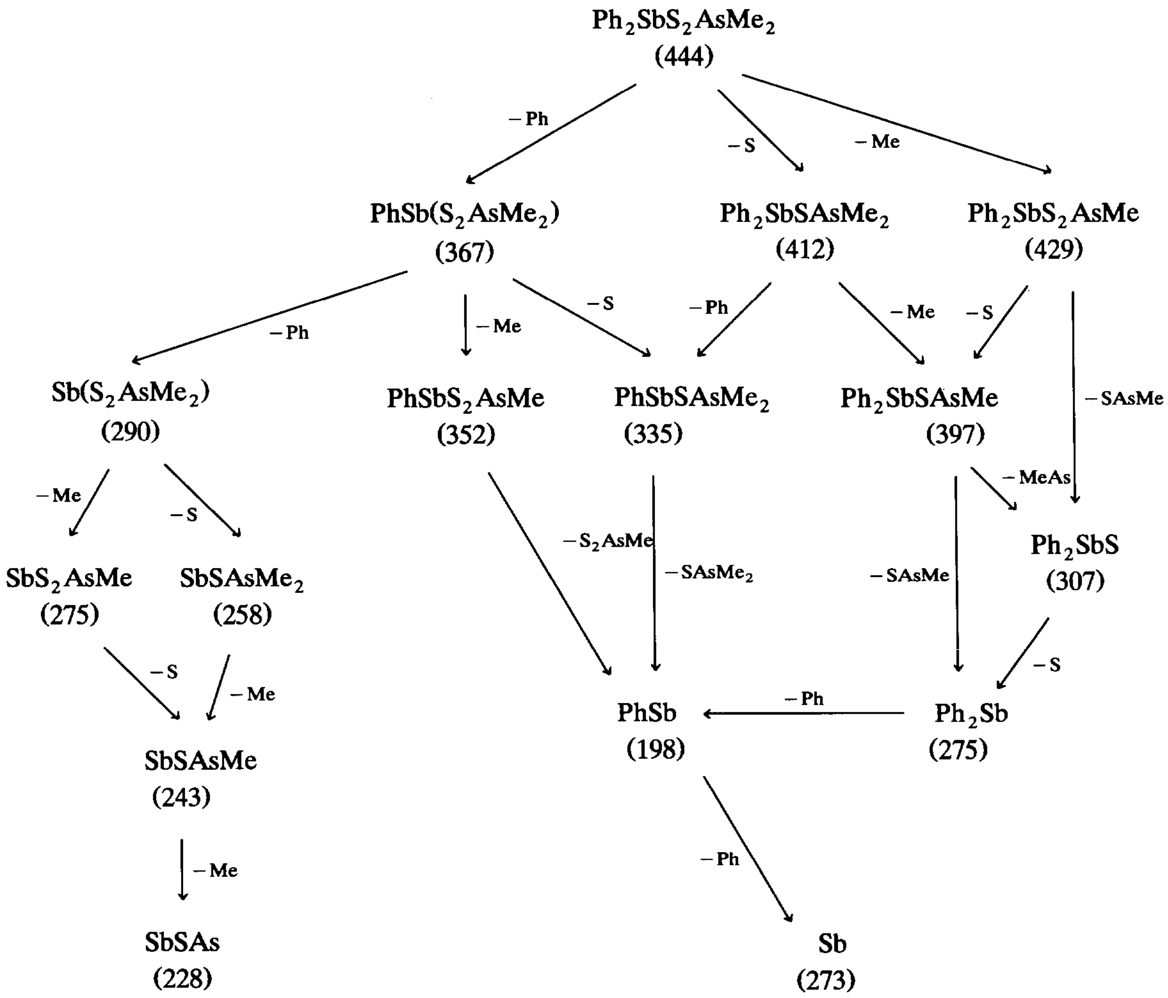

Scheme 3. FAB mass spectrum of $Ph_2SbS_2AsMe_2$.

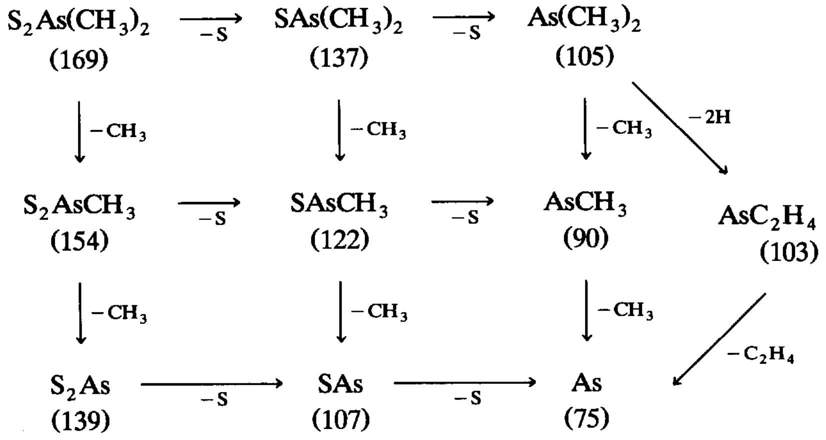

Scheme 4. Fragmentation of the dimethyldithioarsinate group.

TABLE 3. Relative intensities of the antimony-containing fragments in the FAB mass spectra of **1**–**3**

Fragment	m/z (relative intensity)		
	$Sb(S_2AsMe_2)_3$	$PhSb(S_2AsMe_2)_2$	$Ph_2SbS_2AsMe_2$
$Sb(S_2AsMe_2)_3$	628(1.7)	–	–
$PhSb(S_2AsMe_2)_2$	–	536(0.9)	–
$Ph_2Sb(S_2AsMe_2)$	–	–	444(20.3)
$Sb(S_2AsMe_2)_2$	459(83.7)	459(77.0)	–
$Sb(S_4As_2Me_3)$	–	444(25.9)	–
$Ph_2Sb(S_2AsMe)$	–	–	429(4.9)
$Sb(S_3As_2Me_4)$	427(22.3)	427(16.3)	–
$Ph_2Sb(SAsMe_2)$	–	–	412(5.8)
$Sb(S_2As_2Me_4)$	395(5.7)	395(4.0)	–
$PhSb(S_2AsMe_2)$	–	367(100.0)	367(100.0)
$PhSb(SAsMe_2)$	–	335(23.7)	335(18.8)
Ph_2SbS	–	–	307(21.2)
$Sb(S_2AsMe_2)$	290(22.7)	290(15.0)	290(12.1)
$Sb(S_2AsMe)$	275(13.7)	275(38.5)	275(22.6)
Ph_2Sb		–	275(22.3)
$[(C_6H_4)_2Sb]$	–	–	273(8.7)
$Sb(SAsMe_2)$	258(6.4)	258(8.0)	258(8.7)
$Sb(SAsMe)$	243(6.9)	243(4.7)	243(6.1)
SbSAs	228(7.6)	228(7.9)	228(5.2)
PhSb	–	198(11.3)	198(15.3)

bond lengths are 2.21 Å in $Me_2As–S–As(S)Me_2$ [3], 2.21 Å in $[Ph_2Sb–S–As(S)Ph_2]_2$ [6] and 2.17 Å in $Me_2Sn[S–As(S)Me_2]_2$ [5], while the arsenic–sulfur double bond distances are 2.07 Å, 2.05 Å and 2.089 Å,respectively. The arsenic–sulfur distances in $Ph_2SbS_2AsMe_2$ are therefore intermediate between single and double bond lengths, indicating extensive delocalization of the π-bond system over the S–As–S fragment.

Compared with related compounds (see Table 5), the antimony–sulfur distances in the present compound are somewhat unusual. The very short "intermolecular" Sb(1)–S(2′) distance (2.830 Å) is striking, and can probably be described as a three center four electron bond, similar to that suggested for Te–S bonds [22]. If the short antimony–sulfur bonds are described as primary and the longer ones as secondary, then Table 5 shows that here the primary Sb–S bond (2.655 Å) is significantly longer than those in related compounds, while the secondary bond (2.830 Å), although longer than the primary bond, is much shorter than such bonds in related compounds.

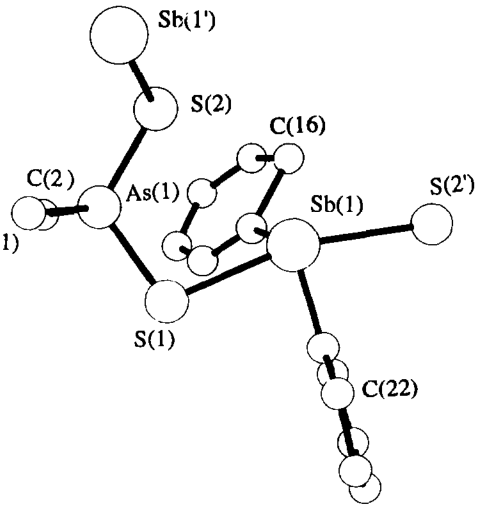

Fig. 1. The basic unit in the structure of $Ph_2SbS_2AsMe_2$, showing the atom numbering scheme.

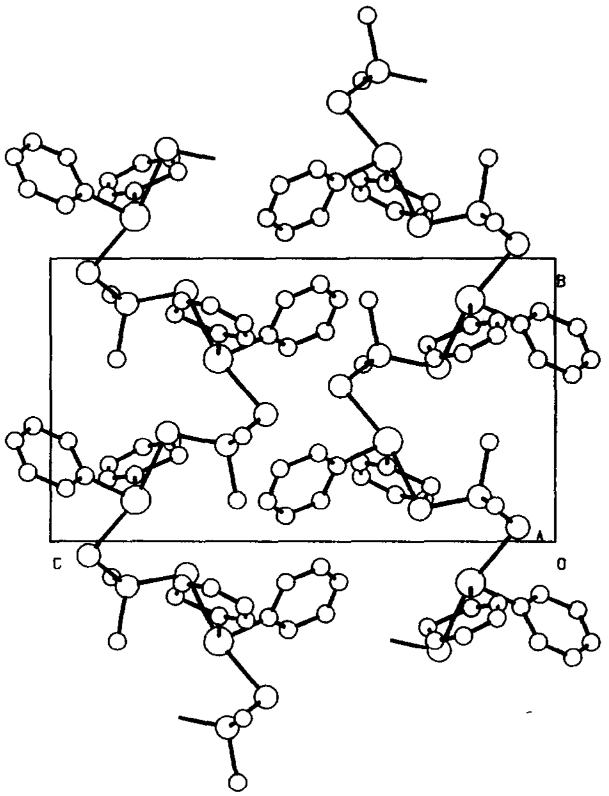

Fig. 2. Projection of the unit cell contents down the *a* axis, showing the polymeric chains.

The geometry around arsenic is slightly distorted tetrahedral, with bond angles in the range 104–114° (see Table 4). The higher value is observed for the S(1)–As(1)–S(2) and S(2)–As(1)–C(2) bond angles. The geometry around antimony is similar to that in $PhSb[S_2P(O^iPr)_2]_2$ [23], but there are differences as illustrated in Fig. 3. Bond parameters for the two compounds are compared in Table 6.

If only primary bonds are considered, the geometry about antimony can be described as trigonal pyramidal, with the Ph(1)–Sb–S(1) ($\alpha = 91.9°$), Ph(1)–Sb–Ph(2) ($\gamma = 97.9°$) and Ph(2)–Sb–S(1) ($\nu = 84.5°$) bond angles close to 90°. However, the secondary interactions cannot be ignored and the coordination geometry around antimony should be regarded as distorted square pyra-

TABLE 4. Bond lengths (Å) and angles (°) for $Ph_2SbS_2AsMe_2$ (with estimated standard deviations in parentheses) [a]

Sb(1)–C(11)	2.151(9)
Sb(1)–C(21)	2.148(9)
Sb(1)–S(1)	2.655(2)
Sb(1)–S(2)	3.652(2)
Sb(1)–S(2′)	2.830(2)
As(1)–S(1)	2.146(3)
As(1)–S(2)	2.124(3)
As(1)–C(1)	1.91(1)
As(1)–C(2)	1.91(1)
C(11)–Sb(1)–C(21)	97.9(3)
C(11)–Sb(1)–S(1)	91.9(3)
C(11)–Sb(1)–S(2)	78.7(3)
C(11)–Sb(1)–S(2′)	89.8(3)
C(21)–Sb(1)–S(1)	84.5(2)
C(21)–Sb(1)–S(2)	151.3(2)
C(21)–Sb(1)–S(2′)	80.8(2)
S(1)–Sb(1)–S(2)	67.29(7)
S(1)–Sb(1)–S(2′)	165.34(8)
S(2)–Sb(1)–S(2′)	127.26(3)
Sb(1)–C(11)–C(12)	122.7(7)
Sb(1)–C(11)–C(16)	118.8(7)
Sb(1)–C(21)–C(22)	121.8(7)
Sb(1)–C(21)–C(26)	118.8(7)
S(1)–As(1)–S(2)	114.5(1)
S(1)–As(1)–C(1)	108.7(4)
S(1)–As(1)–C(2)	104.8(4)
S(2)–As(1)–C(1)	108.0(4)
S(2)–As(1)–C(2)	114.4(4)
C(1)–As(1)–C(2)	106.1(6)
Sb(1)–S(1)–As(1)	101.01(9)
Sb(1)–S(2)–As(1)	74.98(7)
Sb(1)–S(2′)–Sb(1′)	125.33(8)
As(1)–S(2)–Sb(1′)	104.32(9)

[a] Atoms carrying primes are related to unprimed atoms by the symmetry operation $-x$, $y-0.5$, $0.5-z$.

midal. As in $PhSb[S_2P(O^iPr)_2]_2$, the apical position in $Ph_2SbS_2AsMe_2$ (3) is occupied by a phenyl group, but the situation in the two compounds differs in the basal plane. In $PhSb[S_2P(O^iPr)_2]_2$, the basal plane is described by four sulfur atoms of the dithiophosphate ligands. In 3, however, the plane contains two sulfur atoms from the dithio ligand, a third sulfur, S(2′), from a symmetry related molecule and the second phenyl group. The geometry is however strongly distorted, and the base of the pyramid is in fact trapezoidal rather than square.

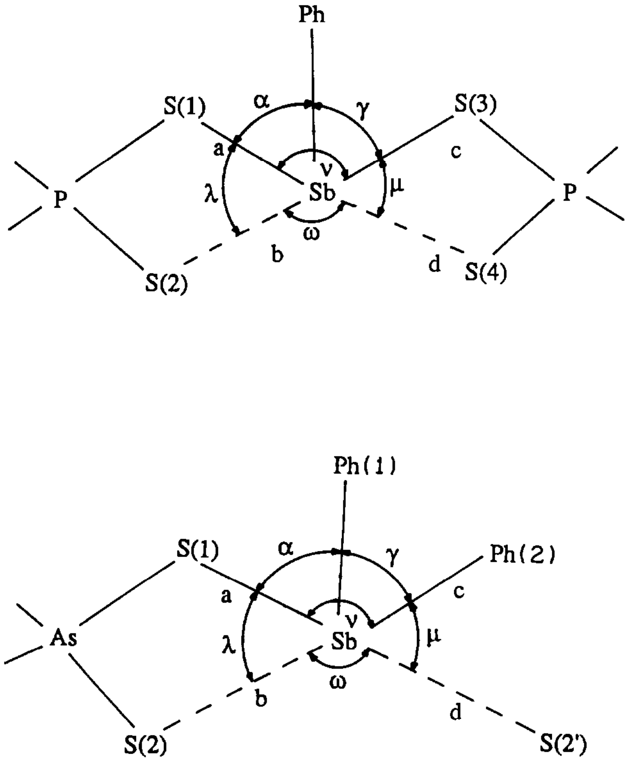

Fig. 3. Comparison of the structures of (a) $PhSb(S_2P(O^iPr)_2]_2$ and (b) $Ph_2SbS_2AsMe_2$.

In $PhSb[S_2P(O^iPr)_2]_2$ this is easy to understand, because the small bite of the two anisobidentate chelating ligands imposes two small S–Sb–S bond angles ($\lambda = 71.51°$ and $\mu = 71.20°$). In 3, the small bite of the dithioarsinate ligand also imposes a small in-plane S(1)–Sb–S(2) bond angle ($\lambda = 67.29°$) but the Ph(2)–Sb–S(2) in-plane bond angle ($\mu = 80.8°$) is remarkably small. In addition, the interligand bond angle S(1)–Sb–S(3) ($\nu = 79.86°$) in $PhSb[S_2P(O^iPr)_2]_2$ is surprisingly close to the corresponding S(1)–Sb–Ph(2) bond angle in 3 ($\nu = 84.5°$). The large S(2)–Sb–S(4) ($\omega = 137.43°$) angle in $PhSb[S_2P(O^iPr)_2]_2$ could be attributed to the strain imposed by the two anisobidentate chelating S_2P

TABLE 5. Comparison of antimony–sulfur bond distances (Å) in $Ph_2SbS_2AsMe_2$, $Ph_2SbSAsPh_2$, and related species.

Compounds	Primary Sb–S bonds	Secondary Sb...S		Type of association	Ref.
		Intramolecular	Intermolecular		
$Ph_2SbS_2AsMe_2$	2.655	3.652	2.830	Polymeric	This work
$Ph_2SbS_2AsPh_2$	2.486	3.471	3.590	Dimeric	6
$Ph_2SbS_2P(O^iPr)_2$	2.531	3.934	3.266	Polymeric	12
$PhSb[S_2P(O^iPr)_2]_2$	2.516	3.056	–	Monomeric	23
$Sb(S_2PPh_2)_3$	av. 2.548	3.029	–	Monomeric	11

TABLE 6. Bond distances and bond angles in $PhSb[S_2P(O^iPr)_2]_2$ and $Ph_2SbS_2AsMe_2$

		$PhSb[S_2P(O^iPr)_2]_2$ (Ref. 23)	$Ph_2SbS_2AsMe_2$ (This work)
Sb–S(1) (Å)	(a)	2.516	2.655
Sb–S(2) (Å)	(b)	3.056	3.652
Sb–S(3)/[Sb–C] (Å)	(c)	2.529	2.148
Sb–S(4)/[Sb–S(2′)] (Å)	(d)	3.067 2.529	2.830
Axial bond angles (°).		96.1	91.9
		87.4	78.7
		96.4	97.9
		84.6	89.8
"In-plane" angles (°)		71.51	67.29
		71.20	80.80
		79.86	84.50
		137.43	127.26

$(O^iPr)_2$ ligands, but there is no obvious reason why the corresponding S(2)–Sb–S(2′) angle ($\omega = 127.26$) in **3** has such a large value. There is no constraint on the position of S(2′), unless the large ω angle in both cases is a function of the presence of a stereochemically active lone pair in the same basal plane. If this is so, then the coordination geometry in both compounds can be described as ψ-pentagonal pyramidal and is related to that found in $Sb(S_2PPh_2)_3$ [11]. The presence of a stereochemically active lone pair in (or very close to) the same plane as the four atoms of the basal plane of the pyramid, rather than below (*i.e. trans* to the apical phenyl group) may seem strange. However, if the three primary (normal covalent) bonds to antimony in these two compounds are considered to describe a trigonal pyramidal, then the positions of both the stereochemically active lone pair and the secondary bonded sulfur atoms becomes less surprising (see Fig. 4) and the small value of μ in **3** (80.8°) is a function of repulsion by the stereochemically active lone pair.

Another structural comparison that deserves comment is that between $Ph_2SbS_2AsPh_2$ [6] and **3**, in which changes in the organic groups remote from the coordination site produce dramatic structural differences. Thus, in the former, monomeric $Ph_2SbS_2AsPh_2$ units dimerize via secondary Sb...S interactions (see Fig. 5), while compound **3** has the polymeric structure described above. Such structural differences produced by remote organic groups are quite common in compounds containing dithiophosphato and dithiophosphinato ligands; *e.g.* $Sb(S_2PPh_2)_3$ has pentagonal pyramidal geometry [11], while $Sb[S_2P(O^iPr)_2]_3$ is distorted octahedral [12], $Ph_2Sb[S_2P(O^iPr)_2]$ is polymeric [10], and $Ph_2Sb[S_2PPh_2]$ dimeric [6].

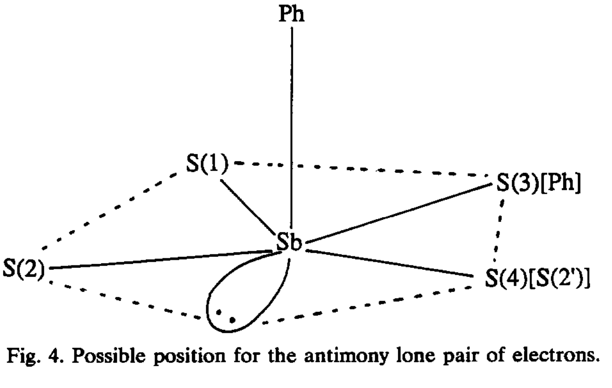

Fig. 4. Possible position for the antimony lone pair of electrons.

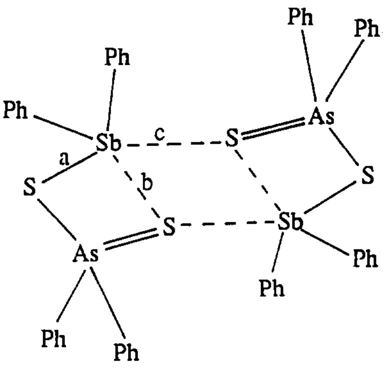

Fig. 5. Dimeric units in the $Ph_2SbS_2AsPh_2$ structure ($a = 2.486$, $b = 3.471$ and $c = 3.590$ Å).

References

1 I. Haiduc, *Rev. Inorg. Chem., 3* (1981) 353.
2 R.C. Mehrotra, G. Srivastava and B.P.S. Chauchan, *Coord. Chem. Rev., 55* (1984) 207.
3 N. Camerman and J. Trotter, *J. Chem. Soc.*, (1964) 219.
4 D. Johnstone, J.E. Ferguson and W.T. Robinson, *Bull. Soc. Chem. Jpn., 45* (1972) 3721.
5 L. Silaghi-Dumitrescu, I. Haiduc and J. Weiss, *J. Organomet. Chem., 263* (1984) 159.
6 C. Silvestru, L. Silaghi-Dumitrescu, I. Haiduc, M.J. Begley, M. Nunn and D.B. Sowerby, *J. Chem. Soc., Dalton Trans.*, (1986) 1031.
7 E.W. Abel, M.A. Beckett, P.A. Bates and M.B. Hursthouse, *Polyhedron, 7* (1988) 1855.
8 L. Silaghi-Dumitrescu and I. Haiduc, *J. Organomet. Chem., 225* (1982) 225.
9 I. Haiduc and L. Silaghi-Dumitrescu, *J. Organomet. Chem., 259* (1983) 65.
10 D.B. Sowerby, I. Haiduc, A. Barbul-Rusu and M. Salajan, *Inorg. Chim. Acta, 68* (1983) 87.
11 M.J. Begley, D.B. Sowerby and I Haiduc, *J. Chem. Soc., Dalton Trans.*, (1987) 145.
12 C. Silvestru, M. Curtui, I. Haiduc, M.J. Begley and D.B. Sowerby, *J. Organomet. Chem., 426* (1992) 49.
13 M. Forster, H. Hertel and W. Kuchen, *Angew. Chem., Int. Ed. Engl., 9* (1970) 811.
14 M. Nunn, D.B. Sowerby and D.M. Wesolek, *J. Organomet. Chem., 251* (1983) C45.

15 D.J. Watkins, J.R. Carruthers and D.W. Betteridge, CRYSTALS *Users Guide*, Chemical Crystallography Laboratory, University of Oxford, UK, 1985.

16 *International Tables for X-Ray Crystallography*, Vol. 4, Kynoch Press, Birmingham, UK 1974.

17 P. Main, S.L. Fiske, S.E. Hull, L. Lessinger, G. Germain, J.P. Declercq and M.M. Woolfson, MULTAN *a System of Computer Programs for the Automatic Solution of Crystal Structures from X-ray Diffraction Data*, Universities of York and Louvain, Belgium, 1980.

18 R.A. Zingaro, K.J. Irgolic, H.D. O'Brien and L.J. Edmonson, Jr., *J. Am. Chem. Soc., 93* (1971) 5677.

19 J.E. Huheey, *Inorganic Chemistry. Principles of Structure and Reactivity*, Harper and Row, New York, 1988.

20 A. Bondi, *J. Phys. Chem., 68* (1964) 441.

21 G. Glidewell, *Inorg. Chim. Acta, 20* (1976) 113.

22 O. Foss, *Acta Chem. Scand., 16* (1962) 779.

23 R.K. Gupta, A.K. Rai, R.C. Mehrotra, V.K. Jain, B.F. Hoskins and E.R.T. Tiekink, *Inorg. Chem., 24* (1985) 3280.